p-Terphenyl-Sensitized Photoreduction of CO_2 with Cobalt and Iron Porphyrins. Interaction between CO and Reduced Metalloporphyrins

T. Dhanasekaran, J. Grodkowski,† and P. Neta*

Physical and Chemical Properties Division, National Institute of Standards and Technology, Gaithersburg, Maryland 20899-8381

P. Hambright

Department of Chemistry, Howard University, Washington, D.C. 20059

Etsuko Fujita*

Chemistry Department, Brookhaven National Laboratory, Upton, New York 11973

Received: April 29, 1999; In Final Form: July 26, 1999

Iron and cobalt porphyrins (FeP and CoP) are utilized as electron-transfer mediators to effect photochemical reduction of CO_2 in homogeneous solutions. The species that activate and reduce CO_2 are the Fe^0P and Co^0P formed by reduction of the starting materials. Reduction of the metalloporphyrins (MP) is achieved by photolysis in dimethylformamide or acetonitrile solutions containing triethylamine (TEA) as a reductive quencher. The photoreduction is efficient for the $M^{III}P \rightarrow M^{II}P$ stage and probably occurs by an intramolecular electron transfer from an axially bound TEA. However, TEA does not bind to the reduced metal complexes, and the quantum efficiency is much lower for the subsequent reduction steps. Considerably higher quantum yields are obtained by adding *p*-terphenyl (TP) as a sensitizer. TP is very effectively photoreduced by TEA to form the radical anion, $TP^{\bullet -}$, which has a sufficiently negative reduction potential to reduce Co^IP and Fe^IP rapidly to their M^0P state. The rate constants for these reactions, determined by pulse radiolysis, are found to be nearly diffusion-controlled. The quantum yield for the reduction of $M^{II}P$ to M^IP and for reduction of CO_2 to CO are increased by more than an order of magnitude in the presence of TP. Side reactions involve hydrogenation of the porphyrin ring and production of H_2. The hydrogenated porphyrins also catalyze reduction of CO_2, but the photochemical production of CO eventually stops. This limit on catalytic activity is due to destruction of the porphyrin macrocycle and accumulation of CO. CO can bind strongly to $Fe^{II}P$ and to Fe^IP but not to Fe^0P, as demonstrated by electrochemical measurements and by optical spectra of the species produced by sodium reduction in tetrahydrofuran in the presence and absence of CO. Although binding of CO to $Fe^{II}P$ and Fe^IP should not interfere with the formation of Fe^0P, the active catalyst, the potential for reduction of Fe^IP to Fe^0P becomes more negative. However, CO probably binds to the hydrogenated products thereby inhibiting the catalytic process.

Introduction

Certain transition metal complexes act as electron transfer mediators for photochemical[1,2] or electrochemical[3] reduction of CO_2. Numerous studies have been carried out on such systems because of the interest in catalyzed reduction of CO_2 as a means of energy storage.[4] Recent studies have shown that iron and cobalt porphyrins are effective homogeneous catalysts for the electrochemical and photochemical reduction of CO_2 to CO and formic acid.[5−7] The mechanism was suggested to involve binding of the CO_2 to the reduced metalloporphyrin in its M^0P oxidation state. In these photochemical studies, the quantum yields for the reduction of the metalloporphyrin and, consequently, for the reduction of CO_2, were relatively low. The present study was aimed at exploring the use of *p*-terphenyl as a photosensitizer for the metalloporphyrin-catalyzed reduction of CO_2 and at deriving the relevant kinetic parameters. The factors that limit the catalytic activity of the present system were also investigated.

Experimental Section[8]

Experiments were carried out with several cobalt and iron porphyrins (MP). The ligands include 5,10,15,20-tetraphenylporphyrins (TPP), tetrakis(3-methylphenyl)porphyrin (TTP), tetrakis(3-fluorophenyl)porphyrin (T3FPP), tetrakis(3-trifluoromethylphenyl)porphyrin ($T3CF_3PP$), tetrakis(pentafluorophenyl)porphyrin (TF_5PP), and octaethylporphyrin (OEP). The complexes were supplied by Mid-Century Chemicals (Posen, IL) in the form of $Co^{II}P$ and $ClFe^{III}P$. The meta-substituted derivatives were preferred to TPP in certain experiments because they are more soluble in acetonitrile and in tetrahydrofuran (THF). *p*-Terphenyl (TP, $C_6H_5-C_6H_4-C_6H_5$) from Aldrich was recrystallized from alcohol. Triethylamine (TEA) was from Aldrich, and acetonitrile (ACN) and *N*,*N*-dimethylformamide (DMF) were analytical grade reagents from Mallinckrodt. TEA and THF were purified as described previously.[7]

† On leave from the Institute of Nuclear Chemistry and Technology, Warsaw, Poland.

10.1021/jp991423u CCC: $18.00
Published on Web 09/04/1999

Irradiations were performed with fresh solutions that were bubbled with Ar or He to remove oxygen or were saturated with CO_2. Photolysis was performed with a 300 W xenon lamp, using a water filter to absorb the IR and a Pyrex filter to absorb $\lambda < 300$ nm. Absorption spectra of the porphyrins were recorded before and after irradiation, the CO evolved was determined by gas chromatography (Carboxen-1000 column, thermal conductivity detector), and the formate produced was analyzed by a Dionex DX-500 ion chromatograph using an AS-11 column and NaOH solutions as eluent. Formaldehyde was analyzed by the chromotropic acid method,[9] methanol, ethanol, and acetaldehyde were analyzed by GC/MS (Hewlett-Packard 5880A gas chromatograph and 5970A mass spectrometer, using a Poraplot Q capillary column at 150 °C) following distillation on a vacuum line. Some of the metalloporphyrins were also reduced using a sodium mirror in THF by standard vacuum line procedures using home-built glassware.[10] An excess of Na was generally used, and the end point of each reduction was carefully monitored by the loss of isosbestic points using a HP 8452A diode array spectrophotometer.

To observe short-lived intermediates and determine rate constants, pulse radiolysis was carried out with the apparatus described previously,[11] which utilizes 50 ns pulses of 2 MeV electrons from a Febetron 705 pulser. Reaction rate constants are reported with their estimated standard uncertainties. All experiments were performed at room temperature, (20 ± 2) °C.

Cyclic voltammograms were recorded with a BAS100B electrochemical analyzer with scan rates ranging from 20 mV s^{-1} to 1 V s^{-1}. A conventional three-electrode system consisting of a Pt or glassy carbon working electrode, a Pt counter electrode, and a standard calomel reference electrode was used. Ferrocene was added as an internal standard at the end of all experiments. All potentials are given with reference to the standard calomel electrode.

Results and Discussion

Kinetics and Mechanisms. The cobalt and iron porphyrins were photochemically reduced in acetonitrile or DMF solutions containing 5% TEA (0.36 mol L^{-1}) as a reductive quencher, as previously described.[6,7] The quantum yield for reduction of Fe^{III}-TPP to Fe^{II}TPP was 0.2 under these conditions, whereas the yields for reduction of $M^{II}P$ to $M^{I}P$ are considerably lower, in the range of 0.01 to 0.04. This difference was ascribed to the fact that TEA binds as an axial ligand to $M^{III}P$ but it does not bind to any significant extent to the $M^{II}P$ or $M^{I}P$ complexes.[6,7] In fact, the UV−vis spectra of $Fe^{II}P$, $Fe^{I}P$, and $Fe^{0}P$ in TEA-containing THF solutions are identical to the corresponding one without TEA. Consequently, photochemical reduction of $M^{III}P$ occurs by an efficient intramolecular electron transfer from the bound TEA to the metal center,

$$Et_3N(Cl)M^{III}P \xrightarrow{h\nu} Et_3N^{\bullet+} + Cl^- + M^{II}P \quad (1)$$

and is followed by reduction of another $M^{III}P$ molecule by the reducing radical derived from TEA.

$$Et_3N^{\bullet+} + Et_3N \rightarrow Et_3NH^+ + Et_2N\dot{C}HCH_3 \quad (2)$$

$$Et_2N\dot{C}HCH_3 + ClM^{III}P \rightarrow Et_2N^+{=}CHCH_3 + M^{II}P + Cl^- \quad (3)$$

On the other hand, photoreduction of $M^{II}P$ and $M^{I}P$ by TEA are less efficient bimolecular processes.

$$M^{II}P + Et_3N \xrightarrow{h\nu} M^{I}P^- + Et_3N^{\bullet+} \quad (4)$$

$$M^{I}P^- + Et_3N \xrightarrow{h\nu} M^{0}P^{2-} + Et_3N^{\bullet+} \quad (5)$$

Moreover, the $Et_2N\dot{C}HCH_3$ radical will reduce $M^{II}P$ more slowly than it reduces $ClM^{III}P$, but it is not likely to reduce $M^{I}P^-$, since the reduction potentials for $M^{I}P^-/M^{0}P^{2-}$ (see below) are more negative than that for the triethylamine radical.[12]

To increase the photochemical reduction yield, we explored the use of *p*-terphenyl (TP) as a sensitizer.[2] This compound has been shown[13] to form an excited state which is rapidly quenched by TEA to produce the radical anion, $TP^{\bullet-}$.

$$TP \xrightarrow{h\nu} TP^* \quad (6)$$

$$TP^* + Et_3N \xrightarrow{h\nu} TP^{\bullet-} + Et_3N^{\bullet+} \quad (7)$$

The reduction potential of the $TP/TP^{\bullet-}$ couple is highly negative (−2.45 V vs SCE in dimethylamine).[13] Since the reduction potentials for Fe^{I}/Fe^{0}TPP (−1.64 V vs SCE)[5] and Co^{I}/Co^{0}TPP (−2.02 V vs SCE)[7] are less negative, $TP^{\bullet-}$ should reduce the metalloporphyrins down to their $M^{0}P$ states.

$$TP^{\bullet-} + M^{II}P \rightarrow TP + M^{I}P^- \quad (8)$$

$$TP^{\bullet-} + M^{I}P^- \rightarrow TP + M^{0}P^{2-} \quad (9)$$

Indeed, we find that the quantum yields for reduction of $Fe^{II}P$ in DMF and $Co^{II}P$ in acetonitrile, both containing 5% TEA, are increased by more than an order of magnitude upon addition of 3 mmol L^{-1} TP to the solution.

Continued photolysis in CO_2-saturated solutions leads to production of CO in a catalytic process. The total yield of CO measured upon photolysis of 0.05 mmol L^{-1} Fe^{II}TPP in DMF/TEA solutions in the presence of 3 mmol L^{-1} TP reached ∼4 mmol L^{-1}, which is ∼6 times higher than that in the absence of TP,[6] and this yield was achieved ∼10 times faster than in the absence of TP. A similar effect is found when comparing the results for Co^{II}TPP in ACN/TEA solutions in the absence of TP (Figure 1a)[7] with those obtained in the presence of TP. Figure 1b shows the results for three concentrations of Co^{II}-T3FPP in the presence of 3 mmol L^{-1} TP. The initial rate of CO production at these three concentrations is about 2 orders of magnitude higher than in the absence of TP.

The considerable increase in the rate of photoproduction of CO indicates that reactions 8 and 9 take place very efficiently. To determine the rate constants for these reactions we used the pulse radiolysis technique. Irradiation of a deoxygenated solution of *p*-terphenyl (0.05 mol L^{-1}) in DMF or DMSO leads to formation of $TP^{\bullet-}$, which has several intense peaks between 400 and 500 nm and between 800 and 920 nm.[13,14] By monitoring the rate of decay at 480 or 840 nm as a function of porphyrin concentration, we derived the rate constants for Co^{II}-TPP, $k_8 = (7.4 \pm 1.2) \times 10^9$ L mol^{-1} s^{-1} in DMSO and $(1.0 \pm 0.2) \times 10^{10}$ L mol^{-1} s^{-1} in DMF. The rate constants for reaction 9 were determined in a similar manner except that the solutions were first photolyzed to reduce the Co^{II}TPP to $Co^{I}TPP^-$ and then pulse irradiated to determine the decay rate of $TP^{\bullet-}$. The values of k_9 were found to be $(6 \pm 2) \times 10^9$ L mol^{-1} s^{-1} in DMSO and $(7 \pm 2) \times 10^9$ L mol^{-1} s^{-1} in DMF. Thus, both reactions 8 and 9 are essentially diffusion-controlled.

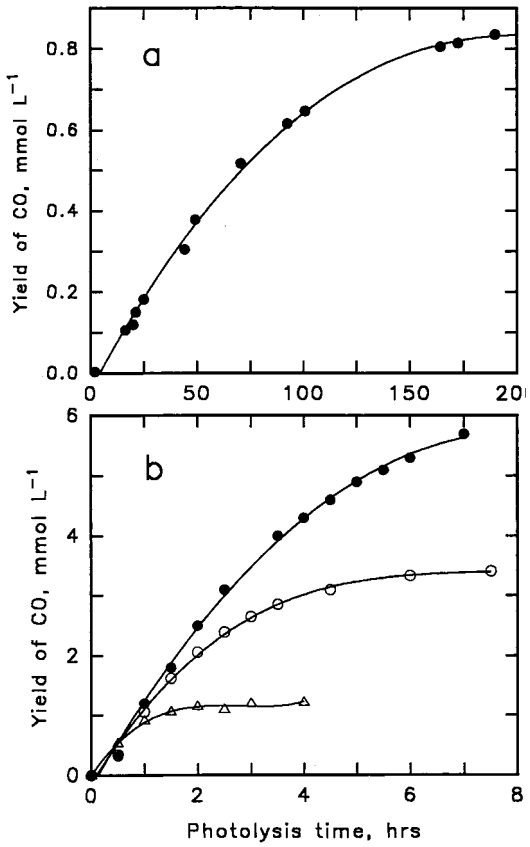

Figure 1. Photochemical production of CO in CO_2-saturated acetonitrile solutions containing 5% TEA and Co porphyrin: (a) 1×10^{-5} mol L^{-1} Co^{II}TPP with no TP; (b) with 3×10^{-3} mol L^{-1} TP and various concentrations of Co^{II}T3FPP, (●) 9×10^{-5} mol L^{-1}, (○) 2.4×10^{-5} mol L^{-1}, (△) 7×10^{-6} mol L^{-1}. The solutions were photolyzed in a Pyrex bulb cooled by a water jacket, placed 10 cm away from an ILC Technology LX-300 UV Xe lamp. The solution volume was 32 mL and the headspace above the solution was 11 mL. The yield of CO in mmol L^{-1} refers to the total amount of CO produced per unit volume of solution.

Saturating these solutions with CO_2 resulted in a lower radiolytic yield of TP$^{\bullet-}$ due to the rapid reaction of CO_2 with e_{sol}^-, which competes with the reaction of TP with e_{sol}^-, but the rate of decay of the remaining TP$^{\bullet-}$ appeared to be unchanged, suggesting that reaction 10 is very slow ($k_{10} \leq 10^6$ L mol^{-1} s^{-1}), as reported before.[2b]

$$TP^{\bullet-} + CO_2 \rightarrow TP + {}^{\bullet}CO_2^- \qquad (10)$$

Nevertheless, this reaction may be expected to take place under certain conditions, since the reduction potential of CO_2 (−2.1 V vs SCE in water)[15] is less negative than that of TP. Despite its low rate constant, reaction 10 may have a contribution in the typical photochemical experiment, since the concentration of CO_2 is at least 3 orders of magnitude higher than the concentration of the metalloporphyrin. It is likely, however, that most of the ${}^{\bullet}CO_2^-$ formed by reaction 10 will react with the metalloporphyrin. Reaction with M^{II}P will take place with a rate constant of the order of 10^8 L mol^{-1} s^{-1} [16] and will lead to reduction.

$$ {}^{\bullet}CO_2^- + M^{II}P \rightarrow CO_2 + M^{I}P^- \qquad (11)$$

Reaction with M^{I}P$^-$ may occur more slowly[7] and form an adduct.

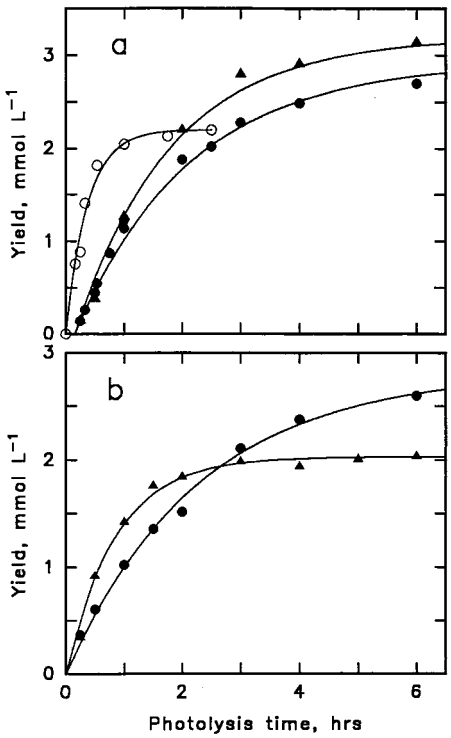

Figure 2. Photochemical production of HCOO$^-$ and CO in CO_2-saturated acetonitrile solutions containing 5% TEA and 3×10^{-3} mol L^{-1} TP. (a) Yield of formate (○) without porphyrin; yield of formate (●) and CO (▲) with 1×10^{-4} mol L^{-1} CoTTP. (b) Yield of formate (●) and CO (▲) with 1×10^{-4} mol L^{-1} FeTTP. The solutions were photolyzed in a $1 \times 1 \times 4$ cm^3 optical cell cooled in a water bath, placed 10 cm away from the Xe lamp. The solution volume was 4 mL and the headspace 2 mL.

$$ {}^{\bullet}CO_2^- + M^{I}P^- \rightarrow (CO_2MP)^{2-} \qquad (12)$$

This adduct is equivalent to that formed by reaction of M^{0}P^{2-} with CO_2,

$$M^0P^{2-} + CO_2 \rightarrow (CO_2MP)^{2-} \qquad (13)$$

and will lead to formation of CO.

$$(CO_2MP)^{2-} + H^+ \rightarrow M^{II}P + CO + OH^- \qquad (14)$$

Photolysis of TP in ACN/TEA/CO_2 in the absence of the metalloporphyrin produces considerable yields of formate (Figure 2a), in agreement with previous results.[13] Under these conditions, the TP is rapidly consumed and the production of formate stops. In the presence of the metalloporphyrin, however, the TP is not consumed because reactions 8 and 9 predominate. The yield of formate in the presence of metalloporphyrins is lower than that without metalloporphyrins at short photolysis times, but reaches the same or higher values at longer times. Parts a and b of Figure 2 show the results obtained with CoTTP and FeTTP, respectively. Similar results were obtained with CoT3FPP. The initial decrease in the yield of formate upon addition of the porphyrin to the TP solution is accompanied by a large increase in the yield of CO, which is not produced at all in the absence of the metalloporphyrin. Comparison of the initial slopes of the curves in parts a and b of Figure 2 also shows that the initial rates of photochemical production of CO and formate with FeTPP and with CoTPP are similar.

Factors Limiting the Yields of Products. Catalytic photoreduction of CO_2 to CO and formate by the metalloporphyrins, as seen in Figures 1 and 2 and in many other experiments, slows down and eventually stops after extended photolysis. It should be noted that the original color of the solution changes in the early stages of the photolysis, turning to green (chlorin) after only 10−20% of the CO and formate are produced, and later turning yellowish. Formation of CO and formate continues even after the solution becomes colorless, until eventually the concentrations of products level off. The limit on production of CO and formate may be the result of complete degradation of the porphyrin (see below).

The total amount of CO formed was dependent on the porphyrin concentration (Figure 1b) but not on the TP concentration (varied from 1 to 8 mmol L^{-1}). This indicates that the porphyrin ($\leq$0.1 mmol L^{-1}) is depleted, while the TP (>1 mmol L^{-1}) and certainly TEA (0.36 mol L^{-1}) and CO_2 ($\sim$0.2 mol L^{-1}) are not depleted. We then compared several complexes: FeTPP, $FeTF_5PP$, FeOEP, and FeOECn (octaethylcorrphycene). By using 1×10^{-4} mol L^{-1} of each metalloporphyrin and 3 mmol L^{-1} TP in CO_2-saturated DMF/TEA solutions, we found that the initial rate of photochemical production of CO was similar for all four complexes and the total yield of CO leveled off at $\sim$4 mmol L^{-1} for the TPP and OEP and $\sim$3 mmol L^{-1} for the other two complexes. This indicates that the limitation in the CO production is not strongly related to the structure or the reduction potential of the porphyrin. Comparison of parts a and b of Figures 2 shows that the total yield of CO obtained with CoTTP is $\sim$1.5 times higher than that obtained with FeTTP, although the total yields of formate were comparable with the two porphyrins. As noted above, however, all the Fe and Co porphyrins studied undergo complete bleaching during the photochemical reduction of CO_2 and yet the catalytic process still continues to produce CO for an extended period. It was further noticed that the colorless photolyzed solutions, when exposed to O_2 for several days, became brown-red. The spectra of these oxidized products, however, were different than the spectra of the original porphyrins. They showed a strong peak at 418 nm and a long tail up to 700 nm but no additional peaks. TLC analysis of the products detected no metalloporphyrin. Electrospray mass spectrometric analysis detected little of the original metalloporphyrin (FeTPP, $m/z = 668$) but mostly fragments ($m/z < 400$).

These results indicate that the porphyrin macrocycle is decomposed during the photochemical reduction of CO_2. The observed bleaching is due to a side reaction and arises from protonation of the macrocycle of reduced intermediates. Reduction of $M^{I}P^{-}$ produces $M^{0}P^{2-}$, in which part of the electron density resides on the macrocycle π-system. Reaction of $M^{0}P^{2-}$ with CO_2 leads to production of CO. Reaction of $M^{0}P^{2-}$ with protons, formed via reaction 2, may lead to protonation of the metal center and eventual formation of H_2.[17] In fact, H_2 is detected as an additional product along with CO in all the current experiments. The yield of H_2 was often lower than the yield of CO, but the ratio varied greatly with porphyrin (Table 1) and with conditions (detailed results will be presented in an upcoming publication). In addition to protonation at the metal, partial protonation at the meso or pyrrolic carbons apparently takes place to produce metal complexes with reduced macrocycles. Chlorins are observed among the early products, and it was shown before[6] that iron tetraphenylchlorin also catalyzes the photochemical reduction of CO_2 to CO. Further saturation of pyrrole double bonds will produce bacteriochlorins and isobacteriochlorins, which have significant visible absorptions,

TABLE 1: Photochemical Production of CO and H_2[a]

	initial rate (mmol L^{-1} h^{-1})		yield[b] (mmol L^{-1})	
compound	CO	H_2	CO	H_2
CoTTP	0.45	0.2	3.1	1.6
FeTTP	0.84	0.1	2.1	3.4[c]

[a] Measured in CO_2-saturated acetonitrile solutions containing 5% TEA, 3 mmol L^{-1} TP, and $\sim$0.05 mmol L^{-1} metalloporphyrin. The solution volume was 35 mL and the headspace was 8.4 mL. The estimated standard uncertainties are $\pm$10% for the values of CO and $\pm$20% for H_2. [b] Measured after $\sim$20 h photolysis, when the concentrations of products generally leveled off. [c] Production of H_2 continued while production of CO stopped.

but saturation of the meso positions eventually produces porphyrinogens,[18] which are colorless. It is likely that any of these complexes can be reduced by $TP^{\bullet -}$ to form a species that can catalyze reduction of CO_2. It is known that the colorless porphyrinogens can be oxidized by O_2 to the corresponding porphyrins but that products saturated at the pyrrole double bonds are not readily oxidized by O_2. The fact that the oxidized products in our experiments are only fragments of the original porphyrins may be due to fragmentation of the macrocycle during the reduction process[19] or during the slow air-oxidation process.

If the hydrogenated metalloporphyrins continue to catalyze the reduction of CO_2, then the limit on the CO yield may be due also to accumulation of products. Two products accumulate in these solutions which may have an effect on the catalytic reaction, namely CO and acetaldehyde. Acetaldehyde is produced by oxidation of TEA and hydrolysis of the imine product[20] (formed for example by reaction 3). Product analysis after extensive photolysis showed the presence of acetaldehyde as well as ethanol. This indicates that part of the acetaldehyde produced in this system is reduced to ethanol. In principle, acetaldehyde may be reduced by $TP^{\bullet -}$ or by $M^{0}P^{2-}$. We carried out pulse radiolysis experiments, similar to those described above, and found that the lifetime of $TP^{\bullet -}$ in DMF is not significantly reduced by the addition of 0.05 mol L^{-1} acetaldehyde. We conclude, therefore, that the reaction of acetaldehyde with $TP^{\bullet -}$ is very slow ($k \leq 10^{6}$ L mol^{-1} s^{-1}) and can be neglected in this system.[21] In support of this conclusion, we also find that 0.05 mol L^{-1} acetaldehyde does not affect the quantum yield for photoreduction of $Fe^{II}P$ to $Fe^{I}P^{-}$ in DMF/TEA/TP solutions. However, addition of 0.05 mol L^{-1} acetaldehyde decreases the rate of production of CO by about a factor of 2. Since acetaldehyde is continuously produced in the photolysis, it will accumulate to a steady-state concentration at which its production rate will equal the rate of subsequent reduction. Thus, accumulation of acetaldehyde constrains CO production but is not the major limiting factor, and the results described below indicate that accumulation of CO is the critical limiting factor.

To examine the effect of the CO accumulated in solution, we diminished the CO concentration by increasing the headspace above the solutions. We photolyzed identical volumes of a solution of FeTPP in DMF/TEA/TP/CO_2 in cells with different total volumes. We find that by increasing the headspace above the solution the catalytic reduction of CO_2 continues for longer periods and yields larger amounts of CO (Figure 3). This indicates that if CO is allowed to escape from the solution the catalytic process will continue. In support of this conclusion, we also find that when the above photolyzed solutions are purged with CO_2 again, to remove the accumulated CO, the photochemical production of CO is resumed. Inversely, if a certain amount of CO is introduced into the solution before

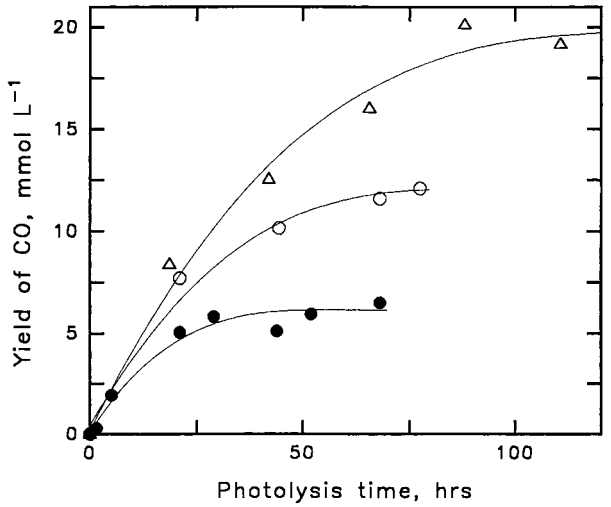

Figure 3. Photochemical production of CO in CO_2-saturated solutions containing 8.6×10^{-5} mol L^{-1} FeTPP, 3×10^{-3} mol L^{-1} TP, and 5% TEA in DMF. The solution volume was 32 mL and the headspace above the solutions was varied: 11 mL (●); 28 mL (○); 52 mL (△).

photolysis, the amount of CO produced by the photolysis is correspondingly diminished.

We then examined whether the concentration of CO levels off because this product is reduced to formaldehyde or methanol in competition with reduction of CO_2. We analyzed the solutions after extensive photolysis but detected no formaldehyde or methanol. We conclude, therefore, that the accumulated CO may interfere with the reduction of CO_2 by binding to the metal ion and preventing the binding of CO_2. It has been suggested before that CO binds to Fe(I) porphyrins[22,23] and that the resulting complex,[22] upon further reduction, is more likely to undergo protonation at the meso position to form the phlorin anion. Consecutive reductions of such complexes in our system may explain the extensive formation of ligand-reduced products. Binding of CO to these reduced complexes may compete with the binding of CO_2 and thus prevent its reduction.

Interaction of CO with the Reduced Metalloporphyrins. To further investigate the effect of CO in these systems, we carried out reduction of iron porphyrins by electrochemical methods and by sodium. Cyclic voltammetry and differential pulse polarography of ClFe^{III}TPP in Ar-saturated butyronitrile solutions show peaks for three one-electron reduction steps, Fe^{III}/Fe^{II}P, Fe^{II}/Fe^{I}P, and Fe^{I}/Fe^{0}P, at −0.26, −1.05, and −1.66 V vs SCE, respectively. Identical reduction peaks are observed in CO_2-saturated solutions; catalytic current is observed at the Fe^{I}/Fe^{0}P reduction step. However, when the solutions were saturated with CO, the Fe^{III}/Fe^{II}P peak became more positive, −0.19 V, the Fe^{II}/Fe^{I}P became more negative, −1.29 V, but the third peak remained unchanged. These shifts are in agreement with previous results[23,24] and indicate that CO binds to Fe^{II}P and to Fe^{I}P, but not to Fe^{0}P. Similar changes take place when THF is used as solvent. Under Ar and CO_2, the potentials for Fe^{III}/Fe^{II}P, Fe^{II}/Fe^{I}P, and Fe^{I}/Fe^{0}P are −0.29 (irr), −1.12, and −1.64 V, respectively. Under CO, they are at −0.3 (irr), −1.35, and −1.64 V vs SCE, respectively. It should be emphasized that CO binding to Fe^{I}P is demonstrated here for unsubstituted TPP in a nonpolar noncoordinating solvent. Addition of TEA to the THF solution does not change the potentials, which indicates almost no interaction between TEA and FeTPP in any oxidation state with and without CO or CO_2. Similar results were obtained with ClFe^{III}T3FPP and ClFe^{III}T3CF$_3$PP (Table 2).

To examine this binding through optical absorption spectra, we carried out stepwise reduction by a sodium mirror in THF

TABLE 2: Reduction Potentials of Iron Porphyrins in *n*-Butyronitrile

porphyrin	potentials[a] vs SCE	$I_p(CO_2)/I_p(Ar)$[b]
ClFe^{III}TPP	−0.26, −1.05, −1.66	2.0
ClFe^{III}T3CF$_3$PP	−0.23, −1.02, −1.61	1.3
ClFe^{III}T3FPP	−0.19, −1.00, −1.55	1.2

[a] Potentials for Fe^{III}/Fe^{II}, Fe^{II}/Fe^{I}, and Fe^{I}/Fe^{0}, with estimated standard uncertainties of ±0.01 V. [b] Estimated standard uncertainties ±15%.

TABLE 3: Spectroscopic Properties of Iron Porphyrins in THF[a]

porphyrin	λ_{max}, nm ($10^{-3}\,\epsilon$, L mol^{-1} cm^{-1})
ClFe^{III}TPP	278 (21.2), 370 (55.4), 416 (112), 506 (13.6), 574 (4.0), 660 (3.0), 688 (3.6)
Fe^{II}TPP	252 (20.4), 294 sh (22.8), 308 (23.5), 426 (241), 540 (11.0), 554 sh (10.5), 598 sh (4.2), 684 sh (1.1)
(CO)Fe^{II}TPP	258 (26.9), 314 (18.5), 414, 534 (12.2), 570 sh (4.3), 610 (2.8)
Fe^{I}TPP^{-}	282 (27.4), 330 (32.8), 394 (67.9), 424 (76.1), 512 (13.8), 572 (7.9), 676 (4.4), 712 sh (3.4)
Fe^{0}TPP^{2-}	254 (27.2), 298 sh (25.0), 358 (66.8), 450 (68.8), 514 (25.2), 710 (5.4), 778 (7.8)
ClFe^{III}T3CF$_3$PP	278 (22.2), 364 (52.8), 414 (109), 505 (12.8), 572 (4.5), 650 (3.2), 678 (3.1)
Fe^{II}T3CF$_3$PP	262 (18.3), 308 (23.6), 366 sh (19.4), 428 (230), 542 (10.2), 600 sh (3.5)
(CO)Fe^{II}T3CF$_3$PP	256 sh (30.5), 320 (25.8), 416 (244), 532 (14.7)
Fe^{I}T3CF$_3$PP^{-}	286 (20.0), 330 (29.5), 394 (44.1), 428 (74.3), 514 (11.5), 578 sh (6.8), 680 (2.7), 712 sh (2.4)
(CO)Fe^{I}T3CF$_3$PP^{-}	254 sh (22.8), 324 (20.6), 396 sh (25.8), 420 sh (46.0), 435 (78.1), 450 sh (46.0), 662 (7.3)
Fe^{0}T3CF$_3$PP^{2-}	256 sh (19.9), 362 (42.6), 452 (51.2), 516 (17.2), 720 sh (3.5), 792 (4.4)

[a] Molar absorption coefficients ϵ were calculated by assuming 100% conversion from the ClFe^{III}P species. Their estimated standard uncertainties are ±10%.

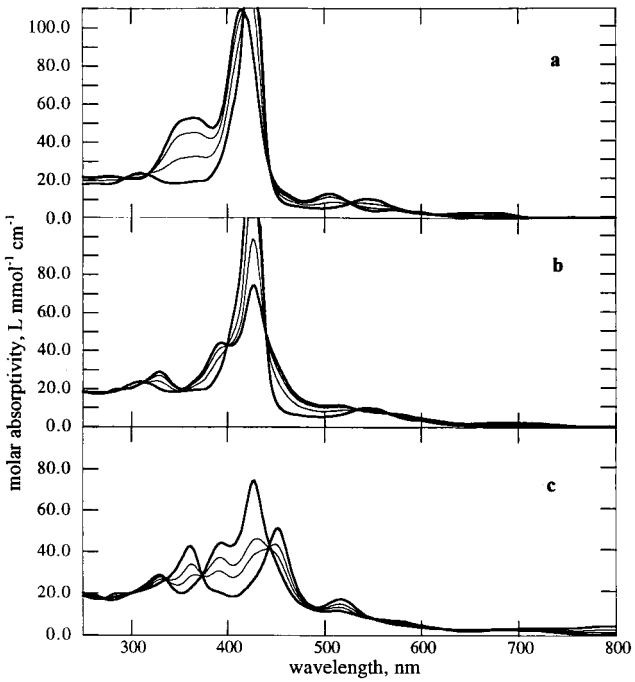

Figure 4. Spectral changes observed upon sodium reduction in THF: (a) reduction of ClFe^{III}T3CF$_3$PP; (b) reduction of Fe^{II}T3CF$_3$PP; (c) reduction of Fe^{I}T3CF$_3$PP^{-}.

solutions of ClFe^{III}TPP and ClFe^{III}T3CF$_3$PP under vacuum. The results are summarized in Table 3. Figure 4a shows the stepwise reduction of ClFe^{III}T3CF$_3$PP (Soret peak at 414 nm) to Fe^{II}-T3CF$_3$PP (Soret peak at 428 nm). Figure 4b shows the stepwise reduction of the reddish solution of Fe^{II}T3CF$_3$PP to the greenish-brown solution of Fe^{I}T3CF$_3$PP^{-} (split Soret at 394 and 428 nm).

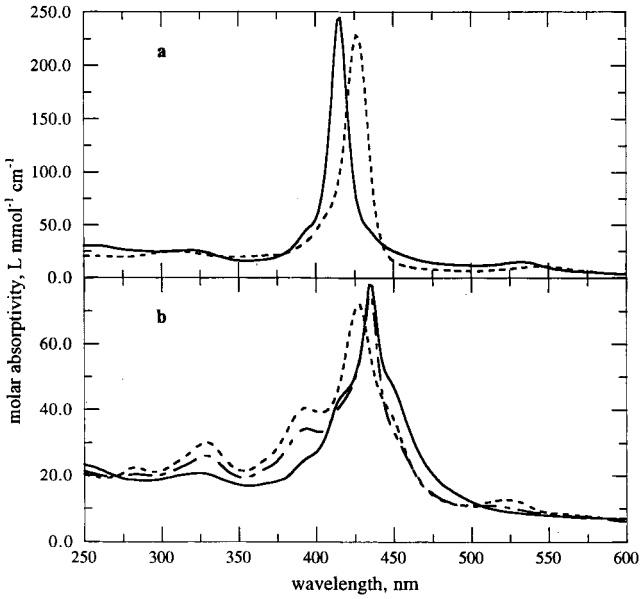

Figure 5. Absorption spectra of $Fe^{II}P$ and $Fe^{I}P$ in THF solutions in the absence and presence of CO. (a) $Fe^{II}T3CF_3PP$ (dotted line) and $(CO)Fe^{II}T3CF_3PP$ (solid line). (b) $Fe^{I}T3CF_3PP^-$ at room temperature (dotted line), $(CO)Fe^{I}T3CF_3PP^-$ at room temperature (dashed/dotted line), and $(CO)Fe^{I}T3CF_3PP^-$ at low temperature (solid line). The $Fe^{I}T3CF_3PP^-$ solution contains trace amounts of $Fe^{0}T3CF_3PP^{2-}$ (shoulder at 450 nm) and of $(CO)Fe^{II}T3CF_3PP$ (shoulder at 416 nm).

Figure 4c shows the stepwise reduction of $Fe^{I}T3CF_3PP^-$ to brownish $Fe^{0}T3CF_3PP^{2-}$ (split Soret peaks at 362 and 452 nm). These changes are similar to those reported for reduction of $ClFe^{III}TPP$.[7,25] Reduction in the presence of TEA produced an identical spectrum at each reduction step, indicating that the interaction of TEA with all oxidation states of FeTPP is not strong.

Addition of CO to solutions of $Fe^{II}T3CF_3PP$ and $Fe^{I}T3CF_3PP^-$ resulted in spectral changes (Figure 5 and Table 3) that indicate formation of $(CO)Fe^{II}T3CF_3PP$ (Soret peak at 416 nm) and $(CO)Fe^{I}T3CF_3PP$ (Soret peak at 435 nm). Addition of CO to a solution of $Fe^{0}T3CF_3PP^{2-}$, however, did not lead to any change in the absorption spectrum even after 2 h, suggesting that this compound does not bind or react with CO. In certain experiments, when the $Fe^{II}P$ was not thoroughly reduced to $Fe^{I}P$, a second peak in the Soret region at 416 nm, with varying intensities, was also observed and was clearly due to $(CO)Fe^{II}T3CF_3PP$ formed along with $(CO)Fe^{I}T3CF_3PP^-$. The solution of $(CO)Fe^{I}T3CF_3PP^-$ can also be obtained from the solution of $(CO)Fe^{II}T3CF_3PP$ by Na mirror reduction under CO. The solution of $(CO)Fe^{I}T3CF_3PP^-$ is thermochromic, brown at room temperature and olive green at low temperature, with the main peak at 436 nm. The spectrum changed reversibly upon raising and lowering the temperature. At room-temperature both $Fe^{I}T3CF_3PP^-$ and $(CO)Fe^{I}T3CF_3PP^-$ exist as an equilibrium mixture ($(CO)Fe^{I}T3CF_3PP^-/Fe^{I}T3CF_3PP \approx 1$ under 1 atm of CO). At low temperature, the solution contains only $(CO)Fe^{I}T3CF_3PP^-$. The binding of CO was fully reversible and the spectrum reverted to that of $Fe^{I}P^-$ upon removal of the CO. Further sodium reduction of $Fe^{I}P^-$ under vacuum and of $(CO)Fe^{I}P^-$ under CO yielded the same product, $Fe^{0}P^{2-}$. This leads to the conclusion that CO does not bind to $Fe^{0}P^{2-}$. Under these thoroughly aprotic conditions, the spectrum of the $Fe^{0}P^{2-}$ was identical with or without CO and there was no evidence of phlorin anion formation (observed before[22] under less thoroughly aprotic conditions). The above spectra of the iron porphyrins, with or without CO, were unaffected by the addition of TEA.

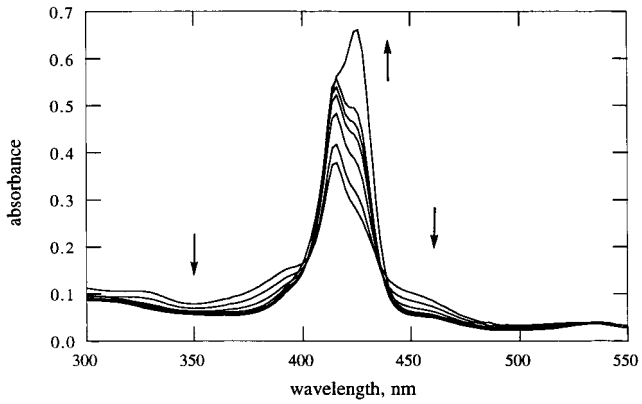

Figure 6. Spectral changes observed with a THF solution of $Fe^{0}TPP^{2-}$ following exposure to 760 Torr of CO_2. The spectra were recorded at 2, 4, 6, 9, 13, 36, and 150 min after the addition of CO_2.

Similar experiments with $Co^{II}TPP$ and $Co^{II}T3CF_3PP$ indicated that CO does not bind to $Co^{II}P$, $Co^{I}P^-$, or $Co^{0}P^{2-}$. This is in contrast to the more saturated tetraazamacrocyclic complexes, where the Co^{I} complexes are known to bind CO.[26] The above results indicate that CO does not interfere with the ability of $Co^{0}P^{2-}$ and $Fe^{0}P^{2-}$ to reduce CO_2, but after the macrocycle is hydrogenated CO may exert a considerable effect on the reactivities of those complexes.

Addition of CO_2 to a THF solution containing $Fe^{I}P^-$ does not cause any spectral change. However, addition of CO_2 to a solution of $Fe^{0}P^{2-}$ immediately produces a $(CO)Fe^{II}P$-like spectrum, with shoulders at 370 and 450 nm, which may be due to the existence of a small amount of $Fe^{0}P^{2-}$ or $(CO_2)Fe^{0}P^{2-}$. Within 10 min, the intensities of the shoulders diminish and the intensity at 414 nm reaches its maximum, indicating the formation of $(CO)Fe^{II}P$, as shown in Figure 6. In the next 2 h, the intensity at 414 nm remains the same but a peak at 426 nm appears and increases, indicating the formation of $Fe^{II}P$. The final solution contains $Fe^{II}P$ and $(CO)Fe^{II}P$ as an equilibrium mixture. Attempts to produce and characterize the $(CO_2)FeTPP^{2-}$ complex by laser flash photolysis failed because of a low quantum yield for the formation of $Fe^{0}TPP^{2-}$ in the $Fe^{I}TPP^-/CO_2$/TEA/THF system. Addition of TP to the system increased the quantum yield of $Fe^{0}TPP^{2-}$, but it caused other complications due to the formation of iron chlorin. Experiments using the more stable phthalocyanines are underway.

Summary and Conclusions

Photochemical reduction of CO_2 to CO is catalyzed by iron and cobalt porphyrins in homogeneous solutions. The metalloporphyrins are reduced to their $M^{0}P^{2-}$ state by photolysis in organic solvents containing TEA, and the $M^{0}P^{2-}$ species reduce the CO_2 to CO. The quantum yields for the photoreduction of the metalloporphyrin and of the CO_2 are greatly increased in the presence of *p*-terphenyl. This compound is photoreduced by TEA very effectively to produce a radical anion, which is found to reduce the metalloporphyrins with diffusion-controlled rate constants down to their $M^{0}P^{2-}$ state. Side reactions in these systems lead to hydrogenation of the porphyrin macrocycle, but these reduced complexes also act as catalysts for reduction of CO_2 until they are decomposed. Acetaldehyde, formed in these solutions by photooxidation of TEA, is found to be reduced to ethanol, and this reduction is in competition with the reduction of CO_2. Accumulation of CO in the solution imposes a limit on further reduction of CO_2. The inhibition effect of CO probably results from CO binding to the metal center thereby competing with the binding of CO_2. Since CO binds strongly

to $Fe^{II}P$ and $Fe^{I}P^{-}$ but not to $Fe^{0}P^{2-}$, $Co^{II}P$, or its reduced states, any $Fe^{0}P^{2-}$ or $Co^{0}P^{2-}$ formed in the solution can react rapidly with CO_2 to form CO. In competition with this process, $Fe^{0}P^{2-}$ and $Co^{0}P^{2-}$ can react with the protons formed by the photolytic reaction. This leads to partial formation of H_2 and partial hydrogenation of the porphyrin ligand. Both of these products are observed. Further hydrogenation of the ligand makes the reduction potentials of the complexes more negative and changes their behavior. It may be speculated that some of these hydrogenated complexes may react with CO_2 in their Fe^{I} and Co^{I} oxidation states, instead of the Fe^{0} and Co^{0} states. Such behavior would be comparable to that observed with the cobalt complexes derived from cyclam and similar ligands.[2] CO binding to the hydrogenated Fe^{I} and Co^{I} complexes may inhibit further CO_2 reduction. Future studies are aimed at examining the properties of the hydrogenated complexes.

Acknowledgment. This research was supported by the Division of Chemical Sciences, Office of Basic Energy Sciences, U.S. Department of Energy, under Contracts DE-AI02-95ER14565 (NIST) and DE-AC02-76CH00016 (BNL). P.H. thanks the Howard University CSTEA project (NASA contract NCC S-184) for financial support. We thank Dr. Bruce Brunschwig (BNL) for helpful discussions and for his participation in the preliminary laser photolysis experiments.

References and Notes

(1) Hawecker, J.; Lehn, J.-M.; Ziessel, R. *J. Chem. Soc., Chem. Commun.* **1985**, 56. Grant, J. L.; Goswami, K.; Spreer, L. O.; Otvos, J. W.; Calvin, M. *J. Chem. Soc., Dalton Trans.* **1987**, 2105. Craig, C. A.; Spreer, L. O.; Otvos, J. W.; Calvin, M. *J. Phys. Chem.* **1990**, *94*, 7957. Kelly, C. A.; Mulazzani, Q. G.; Venturi, M.; Blinn, E. L.; Rodgers, M. A. J. *J. Am. Chem. Soc.* **1995**, *117*, 4911.

(2) (a) Fujita, E.; Brunschwig, B. S.; Ogata, T.; Yanagida, S. *Coord. Chem. Rev.* **1994**, *132*, 195. (b) Ogata, T.; Yanagida, S.; Brunschwig, B. S.; Fujita, E. *J. Am. Chem. Soc.* **1995**, *117*, 6708. (c) Matsuoka, S.; Yamamoto, K.; Ogata, T.; Kusaba, M.; Nakashima, N.; Fujita, E.; Yanagida, S. *J. Am. Chem. Soc.* **1993**, *115*, 601. (d) Ogata, T.; Yamamoto, Y.; Wada, Y.; Murakoshi, K.; Kusaba, M.; Nakashima, N.; Ishida, A.; Takamuku, S.; Yanagida, S. *J. Phys. Chem.* **1995**, *99*, 11916.

(3) Fisher, B.; Eisenberg, R. *J. Am. Chem. Soc.* **1980**, *102*, 7361. Sullivan, B. P.; Bolinger, C. M.; Conrad, D.; Vining, W. J.; Meyer, T. J. *J. Chem. Soc., Chem. Commun.* **1985**, 1414. Beley, M.; Collin, J.-P.; Ruppert, R.; Sauvage, J.-P. *J. Am. Chem. Soc.* **1986**, *108*, 7461. Fujita, E.; Haff, J.; Sanzenbacher, R.; Elias, H. *Inorg. Chem.* **1994**, *33*, 4627.

(4) *Catalytic Activation of Carbon Dioxide*; Ayers, W. M., Ed.; ACS Symposium Series 363; American Chemical Society: Washington, DC, 1988. Behr, A. *Carbon Dioxide Activation by Metal Complexes*; VCH: Weinheim, 1988. *Electrochemical and Electrocatalytic Reactions of Carbon Dioxide*; Sullivan, B. P., Ed.; Elsevier: Amsterdam, 1993. Sutin, N.; Creutz, C.; Fujita, E. *Comments Inorg. Chem.* **1997**, *19*, 67.

(5) Hammouche, M.; Lexa, D.; Savéant, J.-M.; Momenteau, M. *J. Electroanal. Chem. Interfacial Electrochem.* **1988**, *249*, 347. Hammouche, M.; Lexa, D.; Momenteau, M.; Savéant, J.-M. *J. Am. Chem. Soc.* **1991**, *113*, 8455. Bhugun, I.; Lexa, D.; Savéant, J.-M. *J. Am. Chem. Soc.* **1994**, *116*, 5015. Bhugun, I.; Lexa, D.; Savéant, J.-M. *J. Am. Chem. Soc.* **1996**, *118*, 1769.

(6) Grodkowski, J.; Behar, D.; Neta, P.; Hambright, P. *J. Phys. Chem. A* **1997**, *101*, 248.

(7) Behar, D.; Dhanasekaran, T.; Neta, P.; Hosten, C. M.; Ejeh, D.; Hambright, P.; Fujita, E. *J. Phys. Chem.* **1998**, *102*, 2870.

(8) The mention of commercial equipment or material does not imply recognition or endorsement by the National Institute of Standards and Technology, nor does it imply that the material or equipment identified are necessarily the best available for the purpose.

(9) Mitchell, J., Jr.; Kolthoff, I. M.; Proskauer, E. S.; Weissberger, A. *Organic Analysis*; Interscience: New York, 1961; Vol. 1, p 286.

(10) Shriver, D. F.; Drezdzen, M. A. *The Manipulation of Air-Sensitive Compounds*, 2nd ed.; Wiley: New York, 1986. Kobayashi, H.; Hara, T.; Kaizu, Y. *Bull. Chem. Soc. Jpn.* **1972**, *45*, 2148.

(11) Neta, P.; Huie, R. E. *J. Phys. Chem.* **1985**, *89*, 1783.

(12) Wayner, D. D. M.; McPhee, D. J.; Griller, D. *J. Am. Chem. Soc.* **1988**, *110*, 132. Armstrong, D. A.; Rauk, A.; Yu, D. *J. Am. Chem. Soc.* **1993**, *115*, 666.

(13) Matsuoka, S.; Kohzuki, T.; Pac, C.; Ishida, A.; Takamuku, S.; Kusaba, M.; Nakashima, N.; Yanagida, S. *J. Phys. Chem.* **1992**, *96*, 4437.

(14) Shida, T. *Electronic Absorption Spectra of Radical Ions*; Elsevier: New York, 1988; p 141.

(15) Schwarz, H. A.; Dodson, R. W. *J. Phys. Chem.* **1989**, *93*, 409.

(16) Baral, S.; Neta, P. *J. Phys. Chem.* **1983**, *87*, 1502.

(17) Bhugun, I.; Lexa, D.; Savéant, J.-M. *J. Am. Chem. Soc.* **1996**, *118*, 3982.

(18) Fuhrhop, J.-H. In *Porphyrins and Metalloporphyrins*; Smith, K. M., Ed.; Elsevier: Amsterdam, 1975; Chapter 14, p 614.

(19) Chatt, J.; Elson, C. M.; Leigh, G. J. *J. Am. Chem. Soc.* **1973**, *95*, 2408.

(20) DeLaive, P. J.; Foreman, T. K.; Giannotti, C.; Whitten, D. G. *J. Am. Chem. Soc.* **1980**, *102*, 5627.

(21) The finding that both acetaldehyde and CO_2 are reduced very slowly by $TP^{\bullet-}$, while the porphyrins are reduced very rapidly, is probably related to the fact that these small molecules undergo a change in geometry upon reduction.

(22) Balducci, G.; Chottard, G.; Gueutin, C.; Lexa, D.; Savéant, J.-M. *Inorg. Chem.* **1994**, *33*, 1972.

(23) Swistak, C.; Kadish, K. M. *Inorg. Chem.* **1987**, *26*, 405.

(24) Croisy, A.; Lexa, D.; Momenteau, M.; Saveant, J.-M. *Organometallics* **1985**, *4*, 1574.

(25) Anxolabehere, E.; Chottard, G.; Lexa, D. *New J. Chem.* **1994**, *18*, 889.

(26) Fujita, E.; Creutz, C.; Sutin, N.; Szalda, D. J. *J. Am. Chem. Soc.* **1991**, *113*, 343.